CLAS-AnalysisNote 2009-106

Normalization study of the EG3 data using the Δ^{++} reaction channel

Authors : Lewis Graham[1], Kijun Park[1,2], Ralf W. Gothe[1]

[1]University of South Carolina, Columbia, South Carolina 29208, USA
[2]Jefferson Lab, Newport News, Virginia 23606, USA

August 16, 2010

Abstract

As part of the broader study of strangeness photoproduction on deuterium, the $\gamma d \to \Delta^{++}\pi^- \to p\pi^+\pi^-(n)$ cross section was extracted to check the normalization and trigger efficiency of the EG3 data set. The data were acquired at Jefferson Lab using the CLAS detector in Hall B. The photon energy covered a range from 1.1 GeV to 5.5 GeV. A preliminary total cross section for Δ^{++} production as a function of energy has been extracted and is compared to world data and a preliminary cross section measurement from the G11 $\gamma p \to \Delta^{++}\pi^- \to p\pi^+\pi^-$ CLAS data. The comparison of the absolute cross sections determined by EG3 and G11 shows an agreement within a maximum uncertainty of 18% between the two sets of data.

Contents

1 Introduction

This paper covers the methods and procedures carried out to perform a normalization and a trigger efficiency study for the EG3 data set using CLAS. The study culminated with the extraction of a normalized Δ^{++} cross section and compared it to another cross section extraction using the G11 data set, where only the 5 GeV photon beam energy data were used that at least partially overlaps with the EG3 triggered tagged energy region .

We chose the $\Delta^{++}(1232)$ for our analysis study in part because it has an easy to identify $p + \pi^+\pi^-$-final state, a large cross section compared to the Δ^0, is not diffractive as the ρ, and can only be produced off the proton in contrast to both the Δ^0 and the ρ.

Along the same guidelines, we analyzed the G11 data set to compare it to our $\Delta^{++}(1232)$ cross section results. The G11 experimental run was optimized to search for various decay modes of the Θ^+ to contribute to the overall study of the pentaquark. G11 is a new cross section analysis taking place at Jefferson Lab, that coincides widely with the EG3 analysis set up and experimental optimization. Like our data, the G11 (1.0 - 5.2 GeV) data were taken with a tagged photon beam, but at a slightly lower maximum energy than EG3 (1.1 - 5.5 GeV). Thus, G11 presents a optimal choice for our comparison in that it is also photoproduction data and the energy ranges are sufficiently overlapping for our study. Furthermore, since EG3's triggered tagged range overlaps with that of G11, we feel a comparison of the $\Delta^{++}(1232)$ cross section from these data sets will suffice to adequately study the normalization and trigger efficiency of the EG3 data over the full energy range.

2 Experiment

2.1 Data taking and optimization

The data used for analysis was obtained in Hall B from December 2004 to January 2005. The total running time was 40 days and was taken using a liquid deuterium target. The target, which was positioned 50 cm upstream of the CLAS center, was 40 cm long and 4cm diameter. Data was processed with the standard CLAS offline software packages [3].

The electron beam energy averaged measurements of 5765.5 MeV and 5768.3 MeV before and after Christmas, respectively. The electron beam is measured by its deflection in a magnetic field to the tagging system after it passed through a radiator with a nominal thickness of 5×10^{-4} radiation length. The standard electron beam current was chosen to be 30 nA, and it was limited by the drift chamber performance. The trigger required a hit in the tagger in the energy range from 4.5 to 5.5 GeV. The Level-1 trigger configuration demanded trigger bits five and six. Trigger bit five was prescaled, and required a coincidence in the TOF system and start counter (ST) in the same sector in at least two

sectors. Trigger bit six required both TOF and ST coincidence in at least three sectors. The CLAS Level-2 trigger was not used in this experiment. The Data Analysis chapter describes all procedures and corrections applied to the data for cross section extraction.

2.2 Data selection

For the analysis, we skimmed the EG3 data set requiring an exclusive data set of 3 particles (two positive tracks and one negative track). The skim contained all particles that fulfilled a 2ns vertex timing cut of all particles and a fast-pion vertex minus tagger timing cut of 2ns. The fast pion vertex timing cut acts on the TOF timing difference of the fastest pion calculated back to the vertex. We also incorporated a missing mass squared cut from 0.7 GeV^2 to 1.2 GeV^2 to ensure exclusivity of our 3 particle selection, which is optimal for the Δ^{++} production. The data is binned in 100 MeV incident photon energy bins. The only additional cuts besides the skim cuts are a refined neutron missing mass cut to identify $\gamma d \rightarrow p + \pi^+\pi^- + (n)$, missing momentum cuts to further enrich exclusive and quasi-free events, and proton momentum cuts to eliminate low-momentum protons that do not originate from Δ^{++} decays. These cuts were loosely implemented not to discard any good events. We extract the experimental yield by fitting the shape of the Δ^{++} invariant mass, which also displays a sizeable residual background.

3 Data Analysis

3.1 Kinematic binning

We have adapted the kinematic binning in the analysis of the EG3 and G11 data to each other to minimize systematic differences in their comparison. It is necessary to decide on the bin size before the simulation is carried out that leads to final physics results, because different or poorly optimized bin sizes will cause unnecessary systematic and statistical errors. Being that EG3 data set is the only existing high energy data set with its energy range adapted to optimal Φ^{--} pentaquark production kinematics, the world data will only cover the low spectrum of the energy range. So our choice in kinematic range and bin size need be more in line with G11 than world data, being that G11 covers the entire untriggered and part of the triggered tagged region of EG3. Considering this point, the chosen photon energy range in which both data sets overlap is 2 GeV to 5 GeV.

In the EG3 analysis the number of kinematic bins is extended to 44 from 1.1 to 5.5 GeV with a bin size of 100 MeV. This bin size and range should yield satisfactory statistics in each bin. The same size and range of the kinematic bins are used for acceptance corrections. The acceptance corrected yields were computed by weighting yield with the inverse of the simulated acceptance.

3.2 Δ^{++} identification

For this analysis, the event selection begins with the identification of the $p\pi^+\pi^-$ final state that feeds the Δ^{++} production, and where the measured proton and π^+ originate from the $\Delta^{++}(1232)$ decay in the gamma-deuteron reaction. Events from the EG3 data set are preselected (called"skim") to contain these Δ^{++} particles. In that, the events have at least one negative (charge conservation) and two positive particles as identified by time-based tracking, this condition is satisfied for the required proton, π^+, and π^- final state. Figure 1 (a) shows $\tau = 1/\beta$ versus momentum in GeV of the two positive tracks and the one negative track for the $p\pi^+\pi^-$ skim set. These are two of several histograms that we used to verify the track selection parameters applied in the skim. Two others are shown on the bottom of Figure 1, displaying the TOF squared mass of all positive and negative particles. As shown in the plots, we clearly see the squared mass distribution of the proton, π^+ and π^-.

The $p\pi^+\pi^-$ skim set contains the requirement for three tracks, a particle vertex time difference of less than $2ns$ and a photon and fast pion vertex time difference of $2ns$. The missing neutron mass squared (MM^2) constraint has in the analysis been refined to $0.8\ \text{GeV}^2 < MM^2 < 0.97\ \text{GeV}^2$. However, more requirements were applied in the offline analysis to improve the Δ^{++} identification. The missing neutron mass squared (MM^2) is displayed in Figure 2. A cut on the missing momentum of 2 GeV enriches the quasi-free production. All these cuts have been applied to both measured and simulated data.

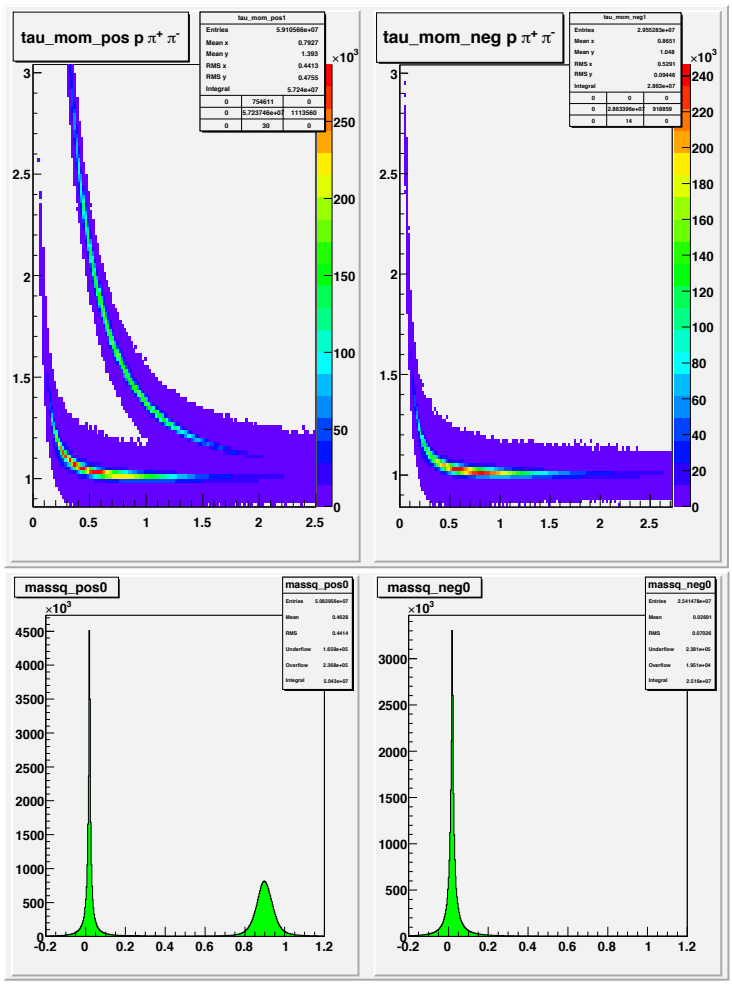

Figure 1: $\tau = 1/\beta$ versus momentum in GeV for positive (top-left) and negative particles (top-right), positive particle TOF mass squared (bottom-left), and negative particle TOF mass squared (bottom-right).

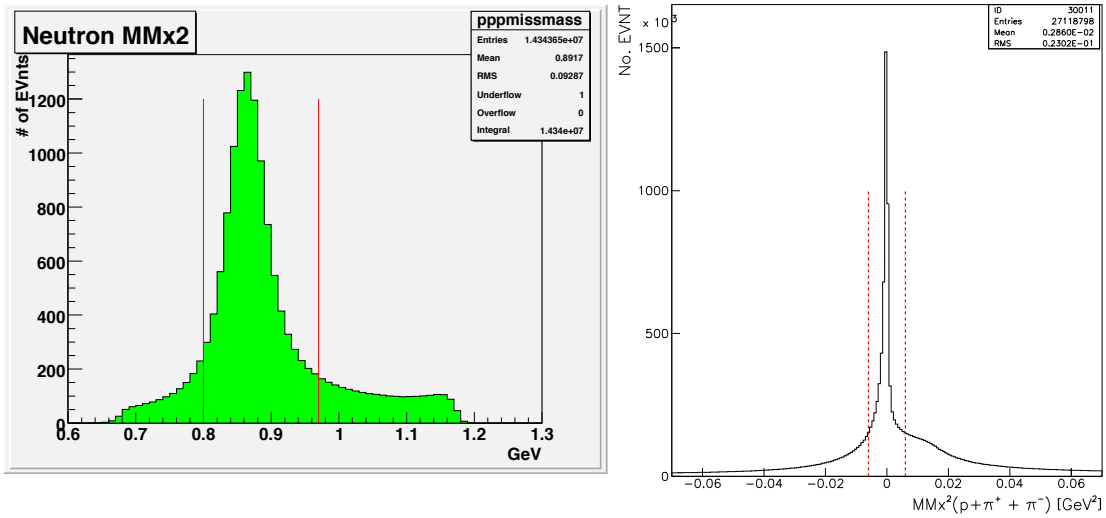

Figure 2: An example of the neutron missing mass squared distribution in GeV^2 for EG3 (left), where the two vertical lines represent the refined cut. And the missing mass squared distribution for G11 (right).

4 Corrections

4.1 Energy loss corrections

Charged particles detected in CLAS may lose a portion of their energy while passing through the target and the detector. This energy loss due to ionization must be accounted for and is corrected in the data set. The exact amount depends not only on the material traversed by the particle, but also the velocity and charge it carries as well as the mass and the vertex. *Eloss* corrections have been applied to the EG3 data set according to the *Eloss* procedure [1].The energy loss corrections are applied to all particles involved in this analysis.

4.2 Momentum corrections

After energy loss corrections are applied, there still exist systematic shifts in the particle momentum determined from CLAS using the standard reconstruction software. These shifts are likely due to the residual effect of imperfect knowledge of the magnetic field and imperfect drift chamber alignment. These shifts can lead to changes to the calculated masses of particles and widening of the peaks when determining their momenta. The procedure was developed to determine the necessary momentum corrections based on particle vertex after energy loss corrections [5]. The resulting momentum corrections are small but have been systematically applied to all charged particles. Their application does not impact the main conclusions of the Φ^{--} analysis [2], meaning that the corrections done to the momentum of the charged particles for this analysis are not affecting the cross section extraction. After applying the corrections, no nominal change should be seen in the momentum distribution for the Δ^{++}.

4.3 Fiducial cuts

We made cuts to the data for the geometrical fiducial volumes. These cuts were made to both simulation and experimental data, where we chose the areas of uniform detector response that can be reproduced by GSIM [8]. The fiducial cuts were studied and formulated by Paul Mattione for 7-momentum bins of positive and negative particles. These cuts were done in the laboratory frame for selected angular ranges. This program has become the conventional way in which fiducial cuts are done in EG3. The fiducial volume cuts are only a function of the momentum and the charge of the particle since the curvature of the particle in a constant magnetic field (the torus was run at a constant inverse field throughout EG3) varies only with the momentum and the charge of the particles. The solid lines in Figure 3 show the standard cut regions employed.

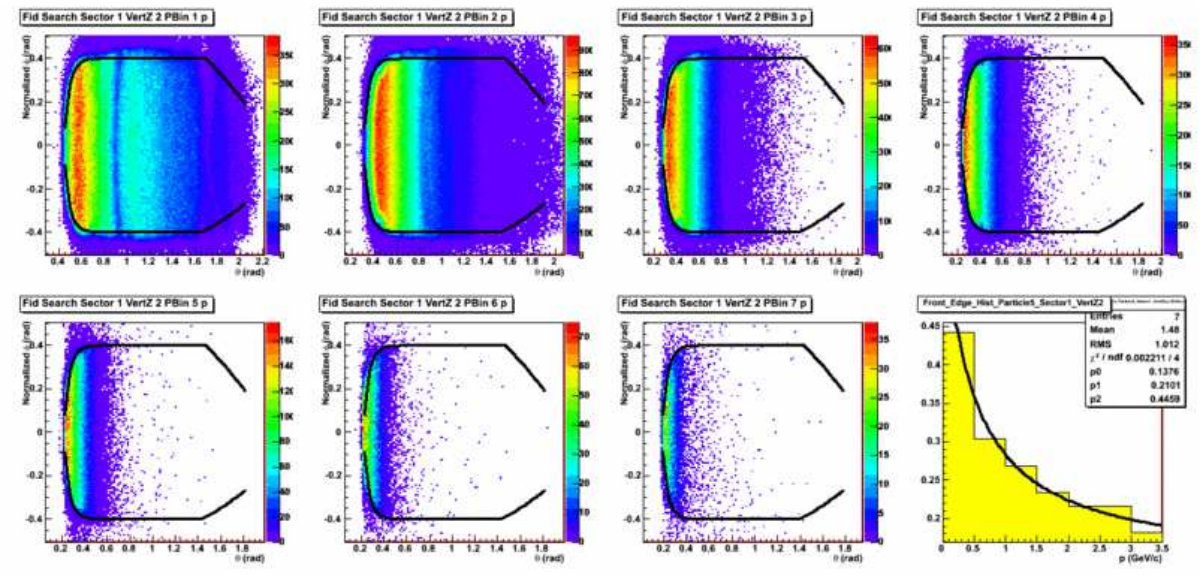

Figure 3: ϕ vs. θ fiducial cut fit for proton in 7 different its momentum bins for sector 1 and the momentum dependent minimum angle(Θ) distribution in the last plot.

4.4 Fitting procedure

We extracted the yields of $\Delta^{++}\pi$ events in each $p\pi^+$ invariant mass bin by fitting the Δ^{++} Breit-Wigner peak and the background contributions. The yields were extracted from fits to the one-dimensional histograms of the $p\pi^+$ invariant mass. The fits assumed a third-order polynomial distribution for the $p\pi^+$ background and Breit-Wigner for the invariant mass of the $\Delta^{++}(1232)$ events. The peak position of the Δ^{++} was a fixed parameter at 1.221 in the fitting function, but the Δ^{++} width was left as a floating parameter. The fitting ranges were adjusted for each energy bin in order to properly fit the background under the peak with a third-order polynomial. The photon energy bin sizes are chosen of $\Delta E = 100$ MeV to accumulate a reasonable population in each $p\pi^+$ mass histogram to perform stable fits, Figure 4 demonstrates that this method provides good result in fitting covering the signal and the background under the Δ^{++} peak.

To check the systematics of the fitting procedure, we also performed a fit where events of $p\pi^+$ are assumed to be distributed according to a Gaussian convoluted Breit-Wigner function of the Δ^{++}. After checking the results of both fitting procedures, the Gauss convoluted Breit Wigner did not provide a result that was notably better. Hence, we chose to continue with the Breit Wigner plus polynomial of third-order. Examples of the fitting results are shown in Figure 4.

In Figure 4, the red line is the Breit Wigner fit on top of the bacakground shown

by the yellow line, which is the third-order polynomial fit. The fitted range was chosen to be able to reproduce the background shape under the peak without developing a full model decription of the $p\pi^+$ mass distribution in the $p\pi^+\pi^-(n)$ final state channel off the deuteron.

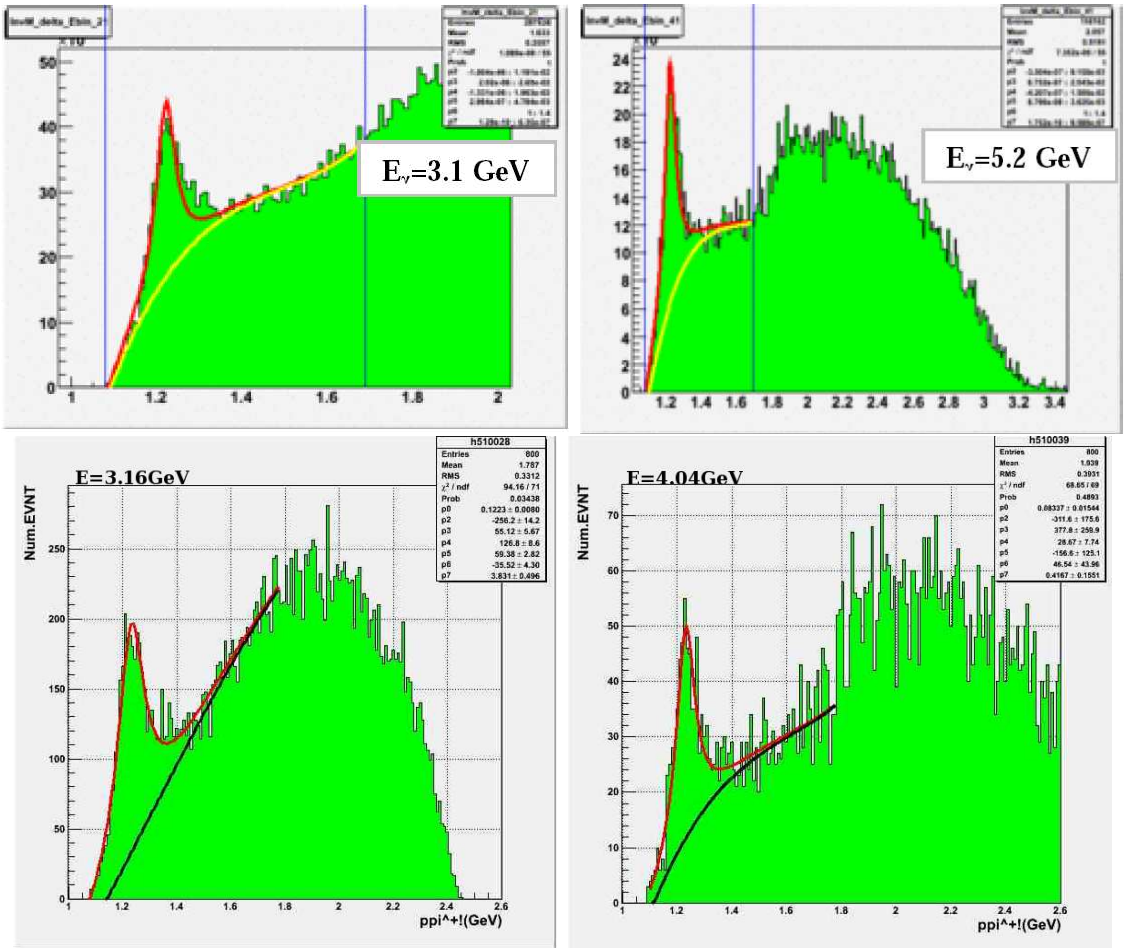

Figure 4: Examples of Breit Wigner plus third-order polynomial fit in terms of the Δ^{++} invariant mass in GeV for EG3 data (top) and for G11 (bottom). Vertical solid lines in each plot show the fitting range.

4.5 Acceptance corrections

In order to calculate the cross section from experimental yields, the acceptance needs to be calculated. For our analysis the components that factor into the acceptance are the detector geometry, the detection efficiency, and the particle reconstruction efficiency. The acceptance was obtained by passing the simulated events through the same reconstruction program used for the measured data, and by calculating

$$Acceptance = \frac{Number\ of\ reconstructed\ events\ in\ a\ bin}{Number\ of\ generated\ events\ in\ the\ same\ bin} \ . \tag{1}$$

To determine the acceptance with sufficient statistical accuracy, 10 million $\gamma d \rightarrow \Delta^{++}\pi^{-}n \rightarrow p + \pi^{+} + \pi^{-} + n$ events were generated using the FSGEN event generator with various t-slopes. The incident electron energy was set to 5.776 GeV to match the maximum electron energy in the experiment, and the photon range was set to 1.1 to 5.5 GeV to coincide with the photon energy range of the experimental data. A study was done with 3 million events to decide the best t-slope choice for the event generator. First simulations were done using a phase space distribution and $t = 0$, but after the study a t-slope of $t = 4$ resulted in the best agreement of simulated and measured Δ^{++} data. Figure 5 shows the corrected measured yields (left) and the generated events (right) fit for t-slope = 4, which showed the best agreement. You can see a slight difference in the slope of the fits for both plots, which led us to an understanding that the t-slope was between 3 and 4. But after careful consideration it was closer to a t-slope of 4. In the reconstructed yields, it is clear that the data point around t = 3 GeV^2 is problematic, but we show the t-slope acceptance calculation in Figure 5 to display from where this discrepancy emerges. In calculating the acceptance, the events drop drastically as you go into higher t bins where the statistical error increases sharply.

The events were then run through GSIM for detector response simulation and the GSIM post processor (GPP) for dead wire drift chamber signal removal and smearing adaptation. After post processing, each file was then processed by RECSIS for reconstruction. Then we calculated the acceptance using the same analysis code with the measured data.

Figure 6 displays the simulated mass for proton-π^{+}. This shows the simulated mass that was produced and binned and fit precisely as the data was binned, where the proton-π^{+} mass of the experimental data are shown in Figure 4. Comparing the two masses it is clear how the simulation provides a clear Δ^{++} peak without the large background seen in the experimental data. The acceptance corrections were applied bin by bin to the experimental data. Each data bin was weighted with an acceptance factor determined by the ratio of reconstructed events to generated events in simulation.

With all completed simulation files we applied the same cuts and corrections used

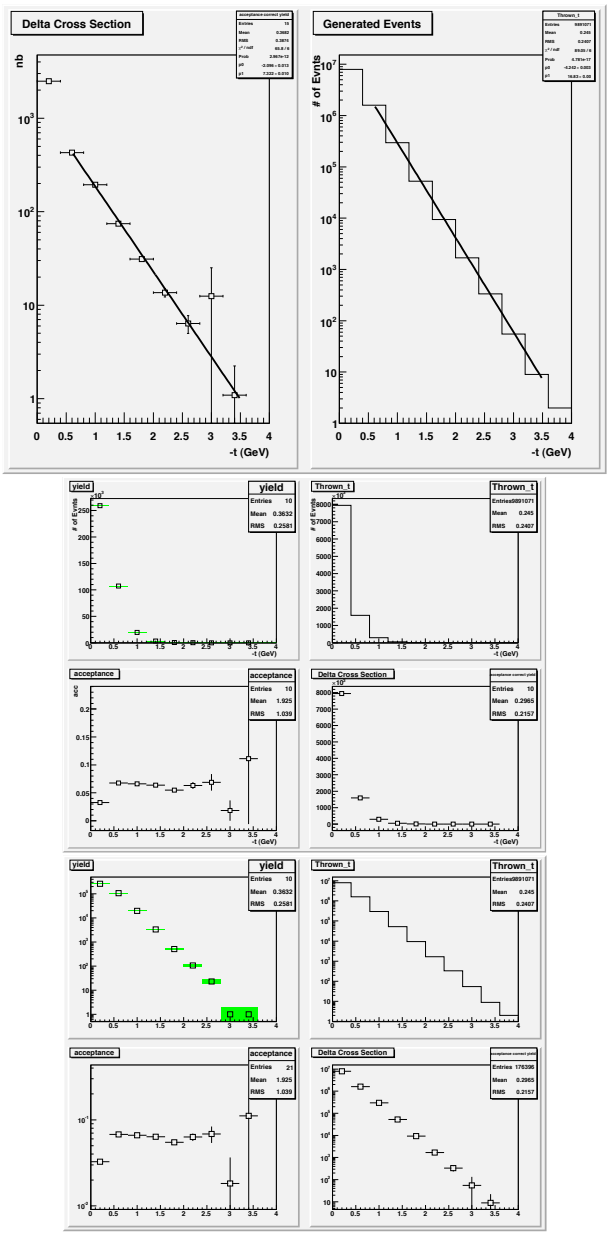

Figure 5: Reconstructed measured and generated t-slope yield events shown versus t in GeV^2 (top plot). Yield, Thrown Events, and Acceptance in linear scale binned in 0.4 GeV^2 of t bins (middle plot). Yield, Thrown Events, and Acceptance in logarithmic scale binned in 0.4 GeV^2 of t bins (bottom plot).

on the experimental data to calculate the acceptance. These include the vertex timing cuts that were made on the skimmed data, the energy binning correction for conversion

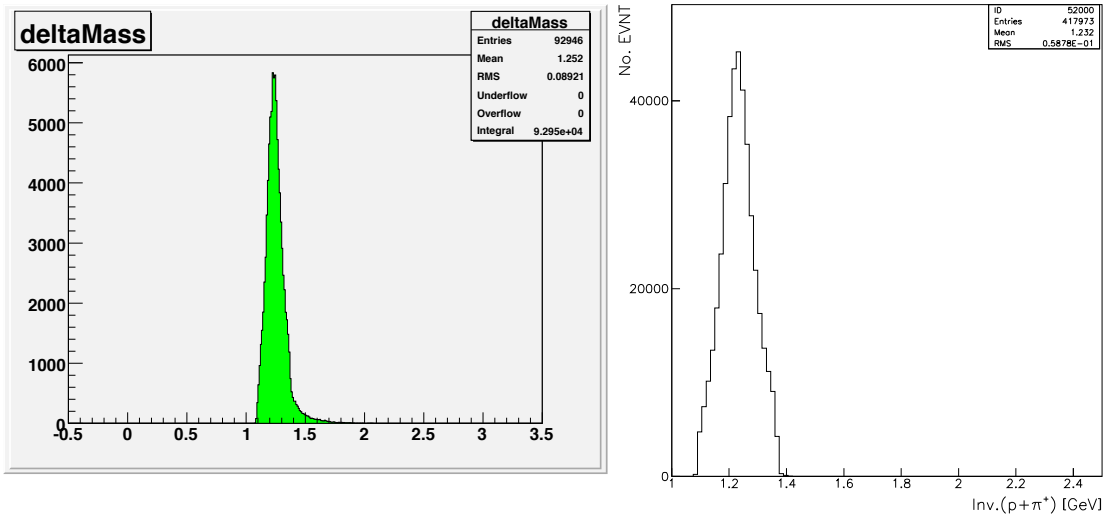

Figure 6: Invariant mass of $p + \pi^+$ in GeV plotted from the simulation for EG3 (left) and G11 (right).

from e-counter bins to energy bins, the neutron missing mass squared cut and the proton momentum cuts. All the corrections were applied to the simulated data in order to achieve reliable acceptance for the selection cuts which were applied as part of the two-pion skim program, thus for final cross section extraction and data evaluation these same cuts must be made on the simulation to achieve an optimal acceptance.

The first cut to the simulated data was the 2ns vertex fast pion timing cut on the difference between the vertex time of the final state particles and the 2ns cut on the difference of the particles' vertex and the photons' tagger times (Figure 7 and Figure 8) display the 2ns cut on the measured data for each set of particles, and then shows the corresponding cut on simulated data for the same particles. We see that the cuts do not take away good events from the simulation but help to ensure that our particle assumptions for particle identification are valid.

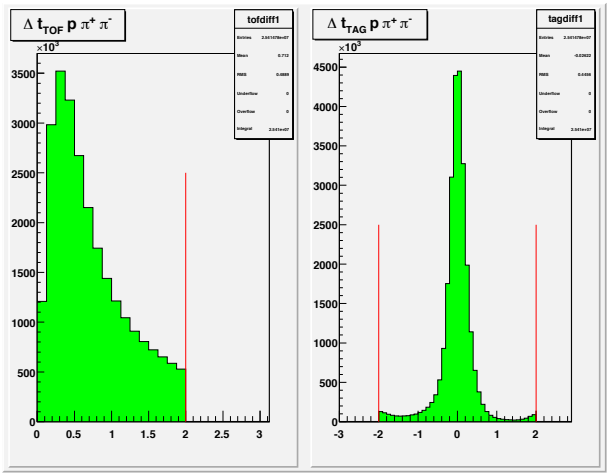

Figure 7: Maximum vertex time difference between the reconstructed particles (left) where the red line shows the cut value. Vertex and tagger time difference between reconstructed particles and tagger photons and $\pm 2ns$ cuts as indicated (right).

Like the vertex timing cut between all particles, we also implemented a timing cut between the particle's vertex time and the photon's tagger time for choosing the right photon for each event. The idea behind this is that if the photon was triggering a good event, then it must be found within the 2ns vertex photon time window for optimal particle identification. Figure 8 displays the 2ns cuts that were applied for vertex and photon time on the skimmed data, and likewise for the simulation.

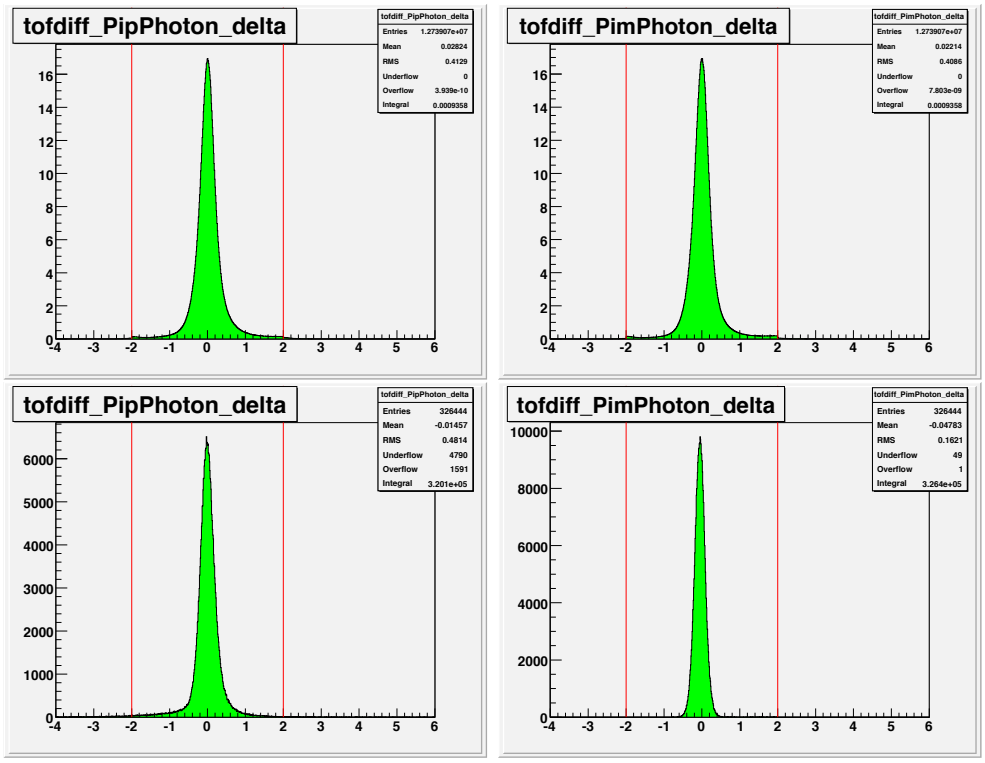

Figure 8: Vertex and photon time difference in ns (π^+ with tagger (right), π^- with tagger (left) plotted from measured (top) and simulated GSIM (bottom) data.

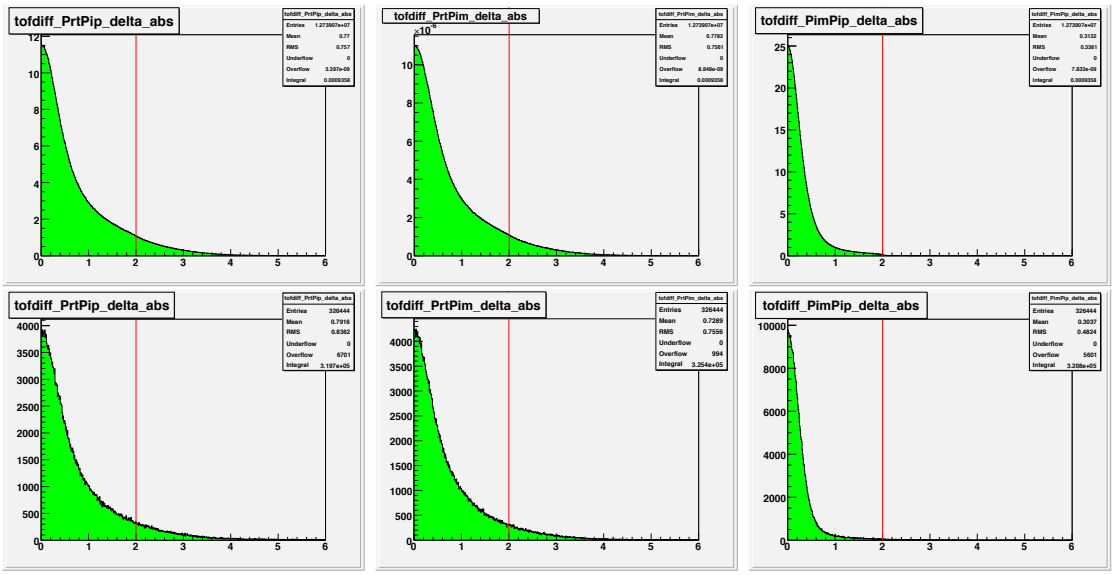

Figure 9: Vertex time difference in ns between the following particle pairs:$p+\pi^-$, $p+\pi^+$ and π^++π^- plotted from the data set for EG3 (top) and simulation GSIM (bottom).

After completing the vertex time cuts, we also took into account multiple photon hits in the tagger. Just using a 2ns vertex time cut to select the good photon is not sufficient in that there may be multiple photons in the tagger. Therefore, we take all photons into account and select the photon closest to the neutron missing mass. The corresponding correction is of the order of 10% and has been applied to the data. Aside from the vertex timing and multiple hits, we incorporated a neutron missing mass squared cut and a proton momentum cut to ensure that we detected good Δ^{++} events and reduce contributions from the background. Our proton momentum cut was limited to 450 MeV and below, as applied to measured and simulated data, and had little effect on protons from Δ^{++} decays.

Figure 10 displays the reconstructed Δ^{++} events (1), the generated events (2) and the resulting acceptance (3) of the ratio of the two plots all plotted against the photon energy in GeV. To accurately gain the acceptance binning must be consistent for both the reconstructed events and the generated events. We obtained a smooth distribution for the acceptance with small statistical and systematic uncertainties.

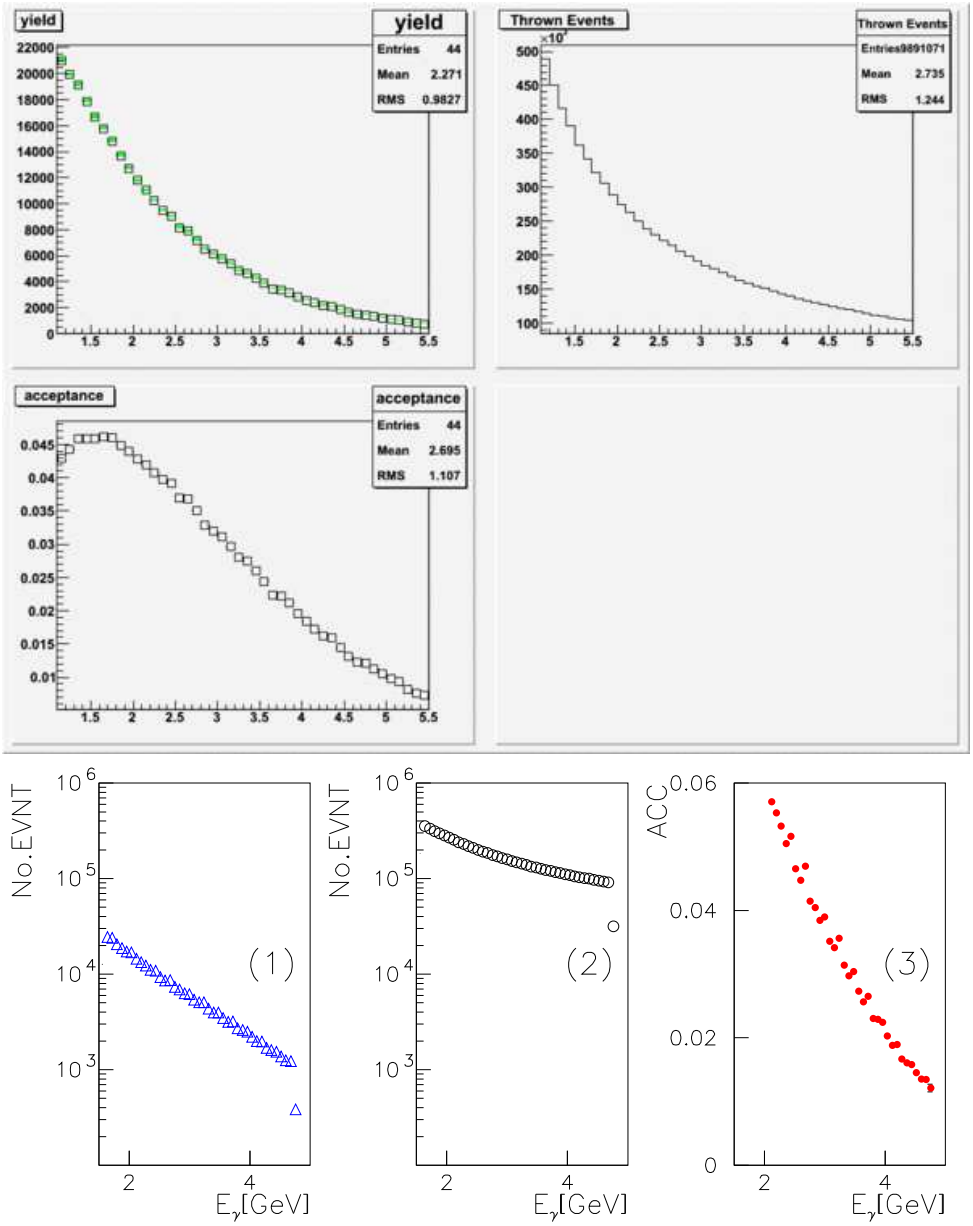

Figure 10: The number of reconstructed events in E_γ [GeV] (1) , the number of generated events (2) and Acceptance (ratio) (3) all from EG3 data (top) and same plots from G11 (bottom).

Figure 11 displays the simulated GSIM data for two reconstructed Δ^{++} events energy bins, 1.5 GeV and 3.1 GeV, each plot shows the mass distribution, where in Figure 6 we showed the $p + \pi^{+}$mass distribution for the entire simulated GSIM events. The Breit-Wigner fit is not needed here, since the simulation has no background contribution and hence all events are taken into account.

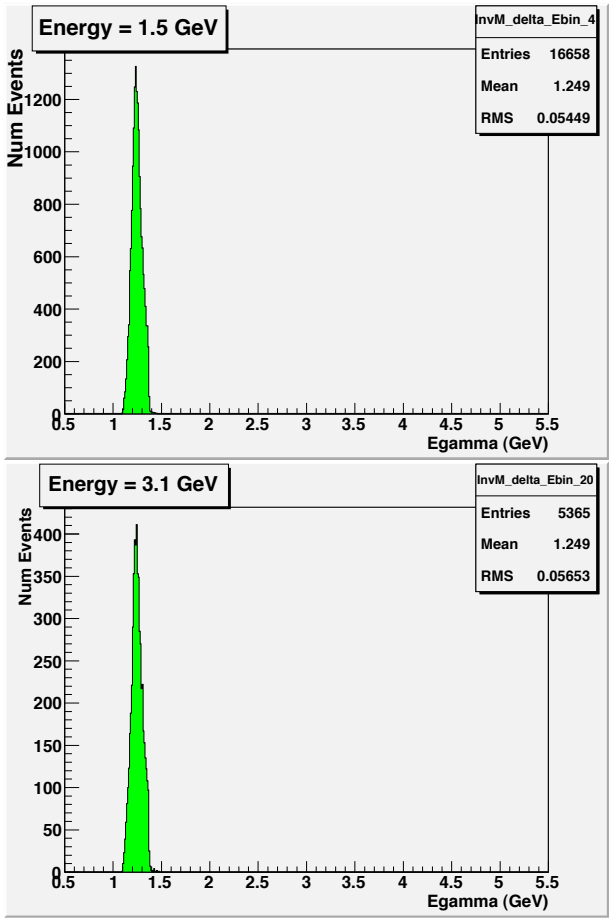

Figure 11: Plots of the GSIM simulated Δ^{++} mass spectrum at two fixed photon energies.

4.6 Normalization

In order to determine the cross section, the data must be normalized to the measured photon flux. This value is normally given by the gflux package, where the number of photons reported by the gflux is already corrected for the acquisition livetime [6] and no further corrections for the deadtime are needed. Figure 12 shows the number of the photons in terms of E-counter bins corresponding to the data sample which was analyzed in this work. This analysis uses the full tagger region corresponding to the energy range of 1.1 to 5.5 GeV. The typical uncertainties are reported by gflux package [2].

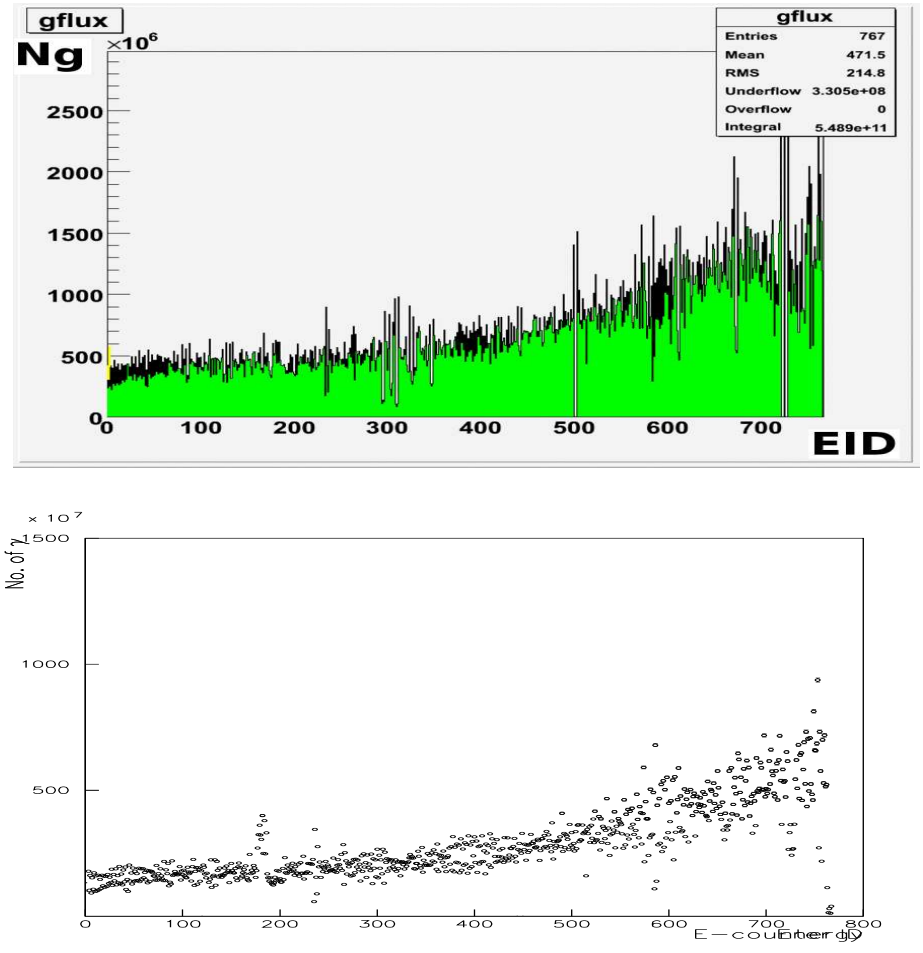

Figure 12: The number of photons in terms of E-counter for an EG3 run (top) and a G11 run (bottom).

4.7 Untriggered tagged event correction factor

The EG3 data set contains a higher tagged energy range than the G11 data set. The G11 data set goes up to 5 GeV where EG3 goes up to 5.7 GeV photon energy. To compare the data sets for the full tagged region that overlaps, we must find a correction factor for the EG3 data for the untriggered tagged region below 4.5 GeV, which causes a step in the yield at 4.5 GeV, where the tagged triggered region begins. The EG3 energy range spans from 1.1 to 5.5 GeV, where the untriggered tagged range is from 1.1 to 4.47 GeV and the triggered tagged range is from 4.48 to 5.5 GeV. Due to accidental coincidences with the tagger, considerable data was acquired in the untriggered region of 2 to 5 GeV. So a correction factor must be found to make the data consistent with the triggered region.

Looking into the correction factor for the untriggered region, if we have an untriggered tagged photon that initiates a good event, it will only be recorded, if an accidental tagged photon in the trigger range occurs within the coincidence time window of the hardware trigger. The hardware trigger is based on the Tagger-Or (MOR) and the Start-Counter-Or (ST) in ASYNC. Thus, we need to know the width of the coincidence gate that triggers an event. For in this gate width an accidental untriggered event is allowed as well.

From the hardware trigger gate we estimate an effective width of this overlap coincidence of $T{=}26.7ns$, which was extracted from an early EG3 test run. The probability for k accidental tagged photons in the trigger window T in dependence of the average rate is given by the Poisson distribution:

$$P_k = \frac{(aT)^k e^{-aT}}{k!} \ , \tag{2}$$

that we also use for the photon flux determination . Thus the probability P for one or more accidental tagged photons in the trigger range is

$$P = 1 - P_0 \ . \tag{3}$$

If we take the average rate of electrons in the trigger range for a nearby EG3 run $a = 13.5 \times 10^6 Hz$, which can be extracted from the gflux files. Then we can estimate a correction factor for the run

$$\frac{1}{P} = 3.30 \tag{4}$$

After extracting the correction factor, it should be applied to the data set for each event. We stress again that this correction factor has to be a constant value according

to the underlying probability theory and we checked that it is indeed run number independent. We now search for a method to extract the overall factor from all runs of the data set. Once the correction factor is applied we have a smooth distribution from the untriggered tagged region into the triggered tagged region as in Figure 14 bottom graphs.

In principle, the theortetical method would be followed to calculate the trigger correction for our data set if we could determine the effective coincidence window with T for all runs from the data, but we chose to use an easier and still fundamental approach to calculate the trigger correction factor. We began to study the gflux normalized events in terms of the E-counters by plotting the photon e-counter spectrum normalized by the gflux for different skims. Since the overall factor has to be constant, we want to investigate the data using the finest possible binning based on the E-counters. Figure 13 was created by using a skim from EG3 devoted to the Lambda production.

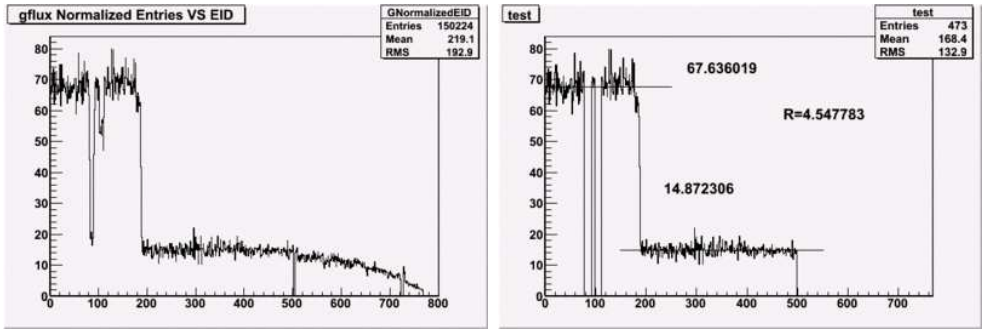

Figure 13: Normalized gflux Entries versus EID and calculated ratio of triggered to untriggered tagged regions.

This skim required at least two charged particle tracks with a narrow mass constraint of 1.098 to 1.133 around the Lambda invariant mass. We chose Lambda production to extract the correction factor being that this is the cleanest (low background) of the EG3 data set, where we can see the jump from the untriggered to triggered range in the plot. From this, we obtain a ratio in terms of the untriggered range of E-counters to the triggered range of E-counters, which gives us the constant correction factor for the tagged untriggered region.

Through further study of this factor, we realized that this factor was channel dependent being that the 4.5 factor extracted from the Lambda skim did not quite complete the correction. We found that once we applied this factor to the $p\pi^+\pi^-$ skimmed data set, it still left the untriggered tagged region slightly short. The reason for this is that the $p\pi^+\pi^-$ is an exclusive skimmed data set where we require only three charged particle tracks (two positive and one negative), where the Lambda was an inclusive skim requiring at least three charged particles. Therefore, we extracted the correction factor from our cross

section plot by raising the untriggered tagged region up to adequately meet the triggered tagged region before our multiple photon hit correction giving us an adjusted factor of 6.4.

Once we extracted the trigger correction factor, we applied it to the data set. Figure 14 shows in linear and logarithmic scales the cross section before and after the implementation of the trigger correction factor.

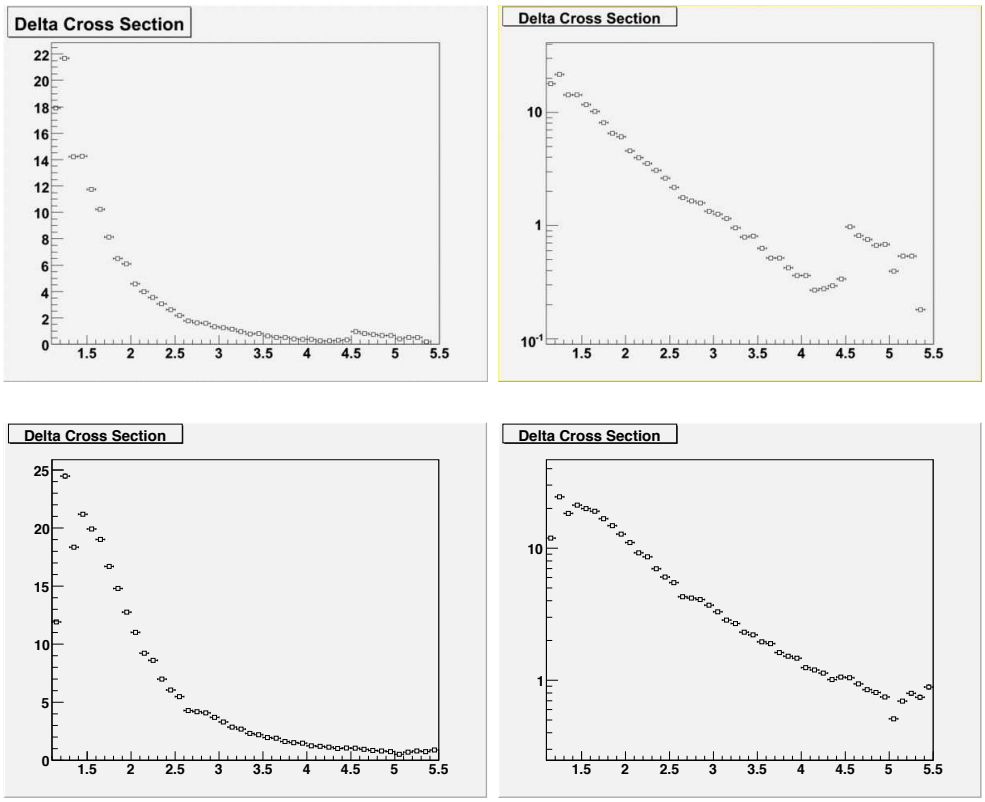

Figure 14: Total cross section in μb of Δ^{++} versus photon energy in GeV without (top) and with trigger correction factor (bottom). Left plots are linear scale and right plots are log scale. The triggered tagger energy range for the EG3 data of 4.48 to 5.5 GeV corresponds to the EID range of 187 to 767. The untriggered tagger energy range is between 1.2 and 4.48 GeV, which corresponds to the EID range of 1-186.

4.8 Trigger efficiency

In the EG3 run, we achieved a luminosity that is exacerbated by the $1/E_\gamma$ dependence of the photon flux where the typical flux in the triggered tagged range is of the order of 3.175e-05 GeV. As documented in the proposal[3], the energy region of interest to EG3 is dominated by multi-pion production. In order to run at the highest luminosity, a trigger scheme must be developed which reduces the rates to a level that can be accommodated by the present DAQ system [3]. It was found during the Φ^{--} analysis, that the yields for four-track events in the three sector trigger were reduced by 20% due to the coincidence between the start counter and the tagger Master OR signals [2].

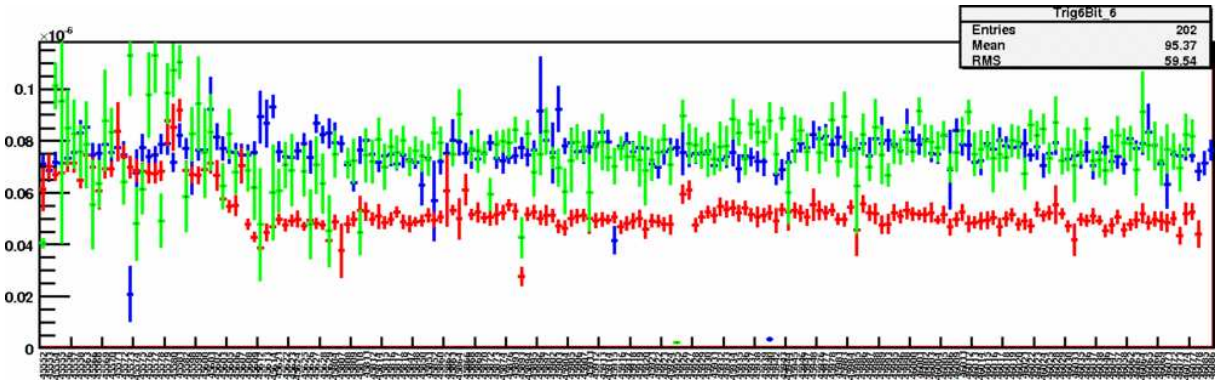

Figure 15: Normalized Yield for Λ vs run number for trigger bit5 and bit6 events.

The normalized rates of $K\Lambda\pi^-$ (4 track, 3 sector events) are plotted versus run number of the data set in Figure 15. Here, the red points are trigger bit 6 (3 sector tracks required) uncorrected, the blue points are trigger bit6 corrected for trigger inefficiency, and the green points are trigger bit5 (2 sector tracks required). The trigger correction for the 4 track, 3 sector events were obtained by the following procedure. Events not in the beam trip interval were utilized, contained a good Λ candidate: ΔT $<$ 0.9ns, DOCA $<$ 3.5cm. It was also require to have at least 3 time based tracks (2 of these are already required for Λ) with a hit in the SC and ST. At least 3 different sectors have to have one of these tracks which is to pick up the first term in bit 6. The events were histogrammed with weights according to the prescale factor (weight is set to 1 for histograms where all bits are taken). Once these requirements were satisfied, then the photon in tagger trigger range was matched within 1 ns window or the photon is assumed if the event is reconstructed. These events were then fit with a gaussian plus a second-order polynomial function. From this, we see that with the 4 track efficiency corrections the 2 sector and 3 sector plotted yields are now in agreement and the correction for trigger bit6 is valid.

This would normally be the entire story to an efficiency study, but the EG3 data set unveiled a critical inconsistency amongst the number of particle tracks we are attempting to correct. In the present study, we performed an efficiency study on our skimmed data set which is based on 3 particle tracks of the proton π^+, and π^- respectively.

We found through this study (Figure 16) a discrepancy in correction to the trigger efficiency of our Δ^{++} cross section. For the Φ^{--} analysis, this efficiency was studied for 4 tracks in 3 sectors in the detector but our analysis requires 3 tracks in 3 sectors.

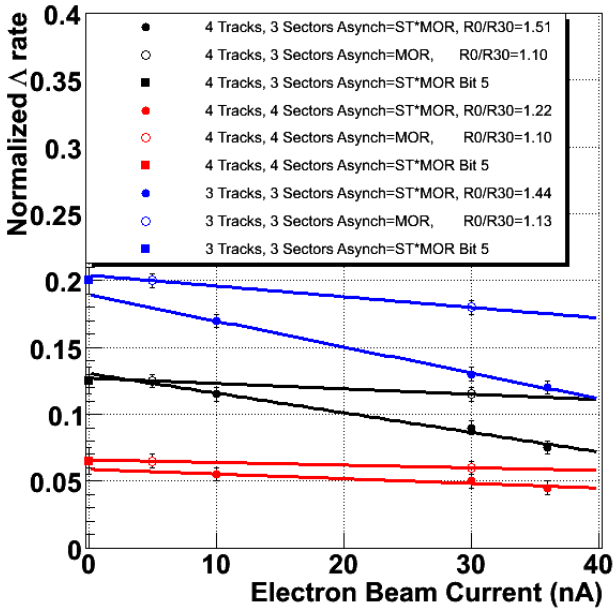

Figure 16: Normalized Λ yield vs beam current for 3 and 4 track events with at least 3 or 4 sector requirements for various triggering methods.

In extracting the Δ^{++} cross section, our first results were drastically off from G11 data and existing published results. In our analysis, we investigated every parameter and process taken to extract the cross section results to recover the missing factors for obtaining a reasonable agreement. What we found through this study is a critical step in the overall analysis of our data. We found through this study a discrepancy in correction to the trigger efficiency of our Δ^{++} cross section. For the Φ^{--} analysis, this efficiency was studied for 4 track in 3 sectors in the detector. However, this analysis requires exactly 3 tracks in 3 sectors, which is the same number as that required in by the trigger.

The correction for the exclusive 3 track, 3 sector channel was investigated by the plots in Figure 17 and 18. Figure 17 shows trigger bit5 events, where the normalized yield of Δ^{++} is plotted for each run versus that run number. The assumption here is that trigger bit5 event for the first 40 runs (before Christmas where coincidence of two sectors was required oopsed to a coincidence of three sectors after Christmas) has 100% efficiency, thus all other triggers should be corrected to the corresponding yield. Thus we fit the average yield for trigger bit5, before Christmas. This fit resulting in the average yield of 0.000211 to be the standard for all triggers. The theory behind this is that because trigger bit5 has 3 tracks but only a 2 sector trigger, there is a greater probablitilty for the particles being detected than in a 3 track 3 sector trigger as the data set requires. Furthermore, in the study of at least 3 tracks the triggered bit5 yield is current independent.

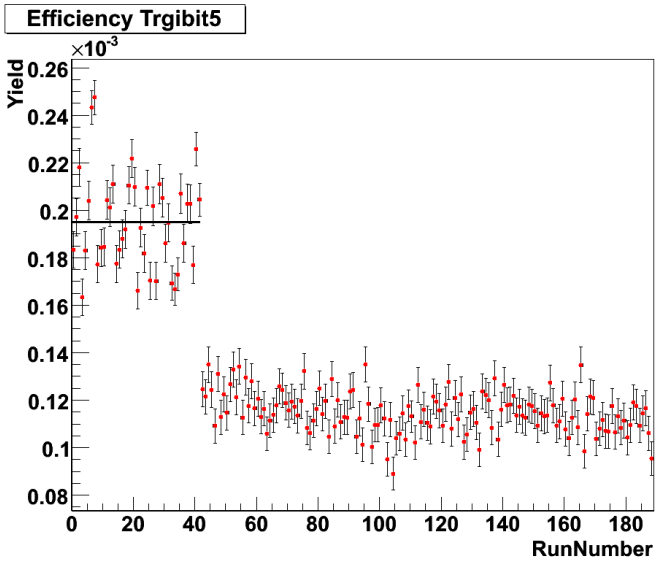

Figure 17: Normalized yield for Δ^{++} vs run number for trigger bit5 events for 0 to 40 (before Christmas) and 41 to 189 (after Christmas). Fit for runs taken place before the coincidence of Start Counter with tagger was instituted for triggering.

Thus, after obtaining the set point for the efficiency, we calculated the efficiency of the Δ^{++} data set which requires a 3 track, 3 sector trigger. Figure 17 and 18 shows the fit for only the range of data before Christmas.

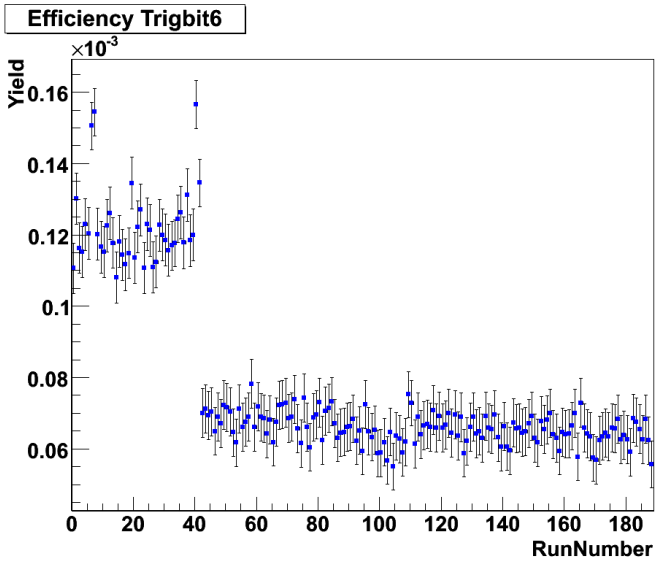

Figure 18: Normalized yield for Δ^{++} vs run number for trigger bit6 events for 0 to 40 (before Christmas) and 41 to 189 (after Christmas).

Likewise, Figure 18 shows the trigger bit6 data before and after Christmas. For each run we obtained the efficiency correction for that run by dividing the trigger bit5 fit value by the yield of the trigger bit6 run. After extracting these efficiency values for each run, we applied these corrections to each run within the analysis code to correct for the overall trigger inefficiency. Table 1 shows the run numbers and the corresponding average of efficiency correction values for those runs before and after Christmas.

Table 1: Average trigger bit6 efficiency correction values for runs before and after Christmas.

RunNumber	Efficiency Correction
45552 - 45627 (coincidence of two sectors)	1.7
45804 - 46113 (coincidence of three sectors)	3.1

For the G11 data set, the G11_prod trigger required a coincidence between Level-1 trigger inputs of CLAS and the tagger-MOR from the trigger logic. The G11 group

defined the Level-1 trigger to require at least two sector-based coincidences between any one of the ST paddles (4) and the TOF paddles (48), where the coincidence contains a time limit window of $150ns$. A coincidence of the tagger MOR and the start counter (OR) within a $15\mu s$ time window was required to reduce the coincidence window amid CLAS and the tagger. This coincidence signal was finally sent to the Level-1 trigger Asynchronous Inputs. The first 6 bits of the Level-1 trigger were then assigned to the 6 sector-based coincidences described above and then put in coincidence with the asynchronous input [7]. Because of possible inefficiencies discovered by the GENOVA group, CMU developed a trigger efficiency map for each particle type as a function of sector, time-of-flight counter and ϕ (azimuthal angle). These corrections to the trigger efficiency were on the 15% level.

5 Results

5.1 Δ^{++} cross section

In order to obtain the cross section, the yield is corrected for all known acceptances and trigger inefficiencies and then normalized by the photon flux. Table 2 outlines all corrections and parameters applied to the EG3 and G11 data sets for the overall cross section comparison. For an adequate comparison study, similar corrections and cuts were made to both data sets.

Table 2: All corrections and cut parameters applied to each data set. Also listed are the average percentages and values of the parameters.

Criteria	EG3	G11 (5 GeV)
Untriggered Tagged Region Correction	5.3 /6.4	-
Timing Vertex Cuts	$2ns$	$2ns$
Photon Time with Tagger Cut	$2ns$	$2ns$
Missing Mass Cut	$0.8 < MM2 < 0.97\ GeV^2$	$\|MM2\| < 0.006\ GeV^2$
Missing Momentum Cut	$MMom < 0.2\ GeV$	$MMom < 0.14\ GeV$
z-vertex Cut	-	$-30cm < vz < 10cm$
Proton Momentum Cut	< 450 MeV	< 500 MeV
Energy loss correction	$< 10\%$	$\sim 10\%$
Momentum correction	$< 2\%$	$< 3\%$
Fiducial volume cuts	applied	applied
Trigger efficiency	38% - 67% [1]	$< 15\%$
Photon flux normalization	$< 2.9 \times 10^{11} >$	$< 4.9 \times 10^{10} >$
Acceptance correction	$\sim 4\%$	$\sim 5\%$
Multiple photon hits correction	$\sim 24\%$	$\sim 15\%$
2ns tagger cut correction	–	$\sim 6\%$

All corrections listed in Table 2 were applied to each set and according to the data run parameter requirements. The only difference shown between the applications is the G11 trigger efficiency study that was applied developed for G11 independent of EG3, and the 2ns tagger and vertex cuts that were only applied to the G11 data. The trigger study

[1] Correction corresponds to the two run periods for the EG3 data. The before Christmas run (no ST in trigger) for trigger bit 6 needs a 38% correction and the after Christmas (ST in trigger) run needs a correction of 67%.

led to a G11 trigger efficiency map that was implemented by CMU to ensure the overall effectiveness. The other difference that surfaced in the data sets was the multiple photon hits correction. This correction was applied to both data sets to account for more than one photon being in the tagger which is used for triggering an event. Once this correction was applied, it was responsible for the cross sections becoming higher for each data set and this is shown in Figure 14 and Figure 19. It is good to mention here that both Figure 14 and Figure 19 also have the trigger correction factor that raises the lower energy which is the dominant component for elevating data below 4.5 GeV. Once all corrections were applied, Figure 19 shows preliminary total cross section of the Δ^{++} binned in photon energy from 1.1 to 5.5 GeV.

The Δ^{++} cross section still contains some inconsistencies below 2 and above 5 GeV that are still being investigated such as the first few data points of the cross section and the last few points. The plot shows a drastic drop in the 1.3 GeV energy bin and 5 GeV energy bin of the cross section which has lead to a E-counter and T-counter calibration study that is ongoing. We believe that these points should be a result of the energy threshold and an incomplete correction through the gflux package as it relates to the E-counter bins. The data above 5 GeV is also being studied where the fitting procedure used must be altered to account for the background under the missing neutron contributing to the invariant Δ^{++} mass peak. The data point at 5.1 was also cut away from the cross section in that it contains an inefficient T-counter which caused the rate to fall lower than the consistent trend of the data. These regions are still under investigation to properly correct them, but hold no correlation to the comparison study of G11 in that our energy range extends further. Thus, for our final comparison we compare the two data sets in the overlap range of 2 GeV - 5 GeV, which checks the efficiency and normalization of the EG3 data.

5.2 Δ^{++} cross section comparison

After getting final results for the Δ^{++} total cross section, our findings were compared to other CLAS data that covered a similar energy range. We chose to compare to G11 data that covers energies up to 4.7 GeV, which extends into the tagged region of our data. Figure 20 shows the Δ^{++} cross section plotted in log scale for the EG3, G11 and SAPHIR published world data. Our analysis study was primarily focused on a comparison of EG3 to G11 CLAS data, but we also included published SAPHIR data to show the low energy agreement as well as to point out the uniqueness of EG3 data in that our data set currently covers the highest energy limit.

In Figure 20, the magenta closed circles represent EG3 data with trigger correction factor respectively. blue open circles is for G11 data. All other red squares are SAPHIR data.

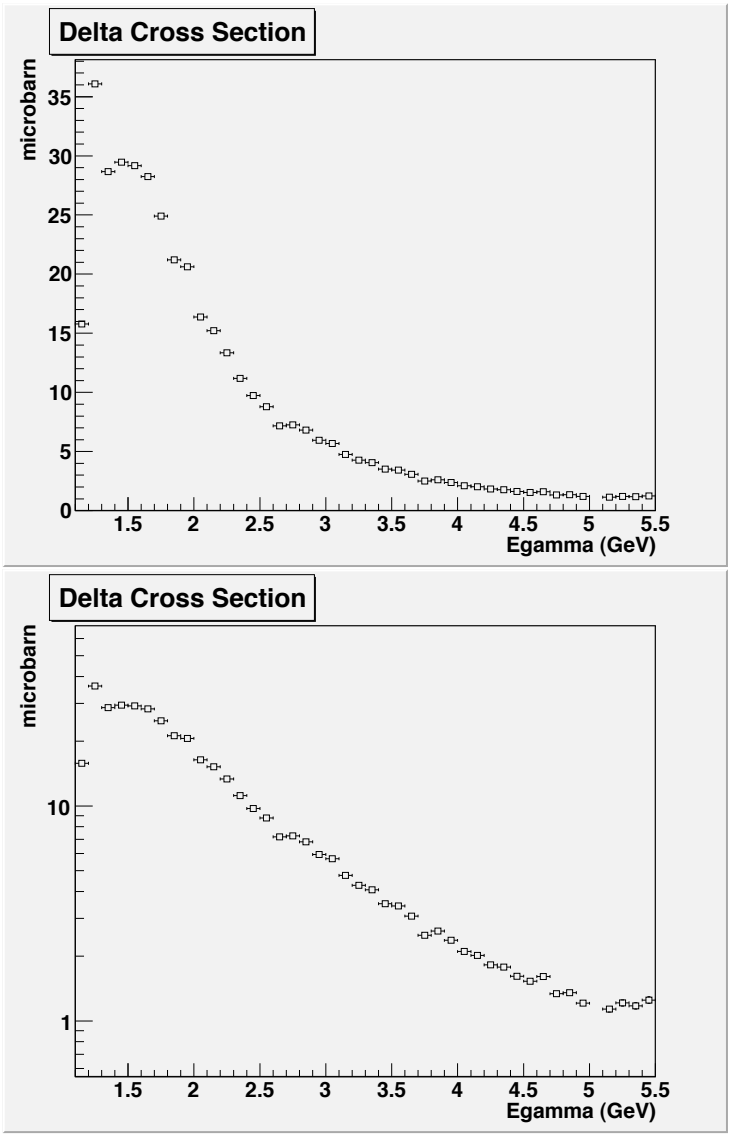

Figure 19: Linear and logarithmic scale total cross section extracted from fits of Δ^{++} invariant mass with acceptance corrections after applying trigger correction factor.

To solidify our results and to obtain an overall difference in the comparison of EG3 to G11, we took the 2 - 5 GeV data points and computed deviations of each data set from an average fit, which is shown in Figure 21. The average fit uses the combined data from EG3 and G11 to a exponent plus a constant as shown in Figure 21. We then calculated the deviations of each of the points from the average fit, as shown in Figure 22, 23 and 24. The deviations from the average fit were themselves fit to a constant which is shown

on each of the figures.

From Figure 28 displaying the average fits to the EG3 and SAPHIR data, and we compare the fit values to estimate the overall difference to be smaller than 10% in the comparison. Figure 23 shows the ratio of EG3 to G11 data fit to the average for the untriggered tagged region data (2 GeV to 4.5 GeV). Figure 24 displays the likewise average fit for the triggered tagged region data (4.5 GeV to 5 GeV). The data sets show good agreement up to an overall maximum uncertainty of 1%. This agreement is predicated upon all corrections and calibrations performed to the EG3 data. In particular, the untagged trigger correction factor was found to be background dependent as previously discussed and is still under further investigation to ensure this finding. Thus we have incorporated corresponding plots for Figures 23 - 28 with the 6.4 trigger correction factor.

Currently, we have found that the correction factor is 6.4 for the fully background converted Δ^{++} cross section to give us the agreement of better than 18% as shown in Table 3 for the exclusive channel utilized in our overall study. We previously assumed a maximum uncertainty between the data sets would be 1% also shown in Table 3, which took into account the untagged trigger correction factor of 5.3 that was originally found in a not fully corrected yield study using the inclusive reaction. Since we have not completed our subtraction of the background under the missing neutron peak, we quote an overall maximum uncertainty of 18% for 6.4. We believe that after the background subtraction study is complete, this will reduce the trigger correction factor back to or within the range of 5.3 and reduce our uncertainty to those values presented in Table 3. Until further studies are carried out, this correction factor marks the maximum uncertainty in the determination of the untagged triggered region correction. We also include Figures 29 - 34 to show the over fits to the slope of the data sets for EG3 and G11.

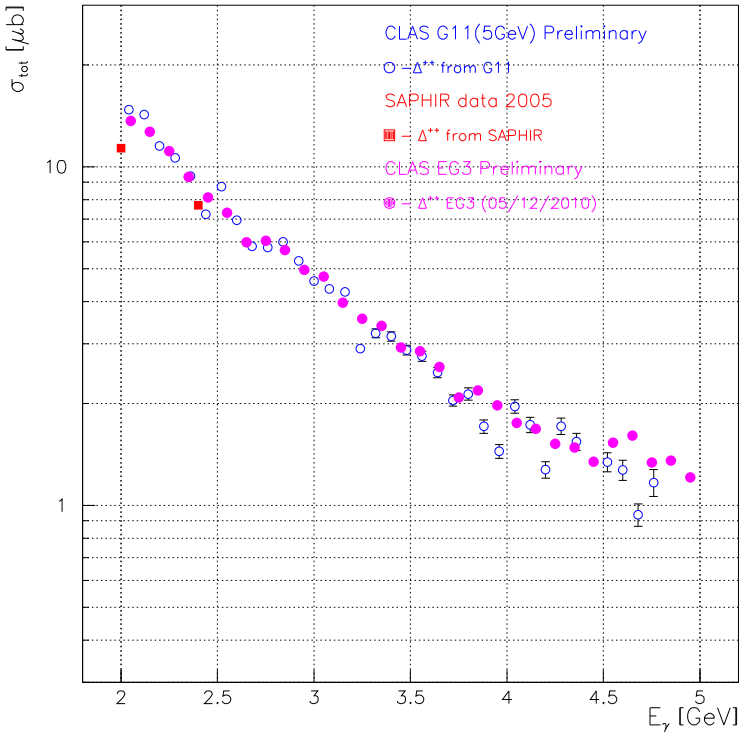

Figure 20: EG3 data (●), G11 data (○) and SAPHIR data (■) total cross section comparisons of the Δ^{++} between 2 GeV and 5 GeV.

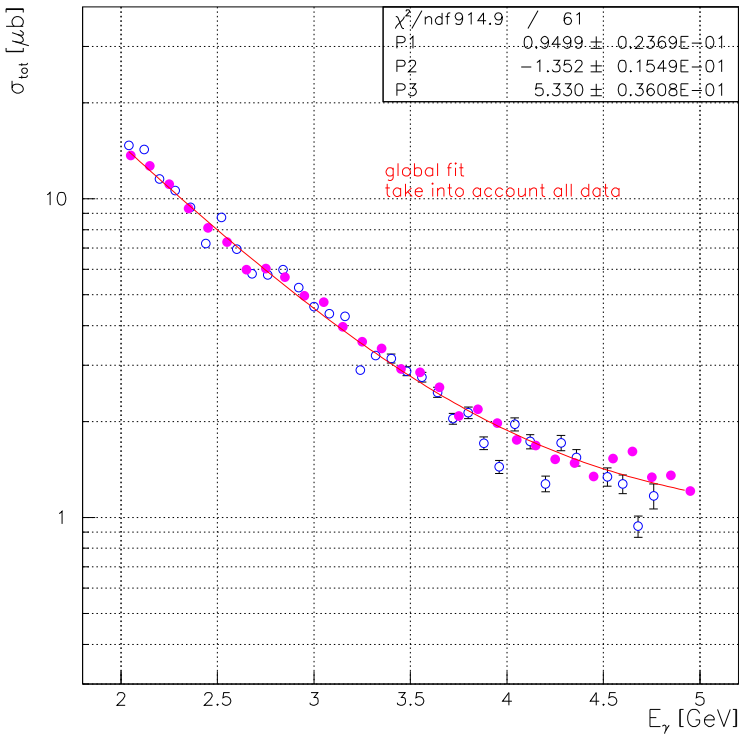

Figure 21: EG3 (•)and G11 (○) total cross section comparison fit of the Δ^{++} between 2 GeV and 5 GeV.

Table 3

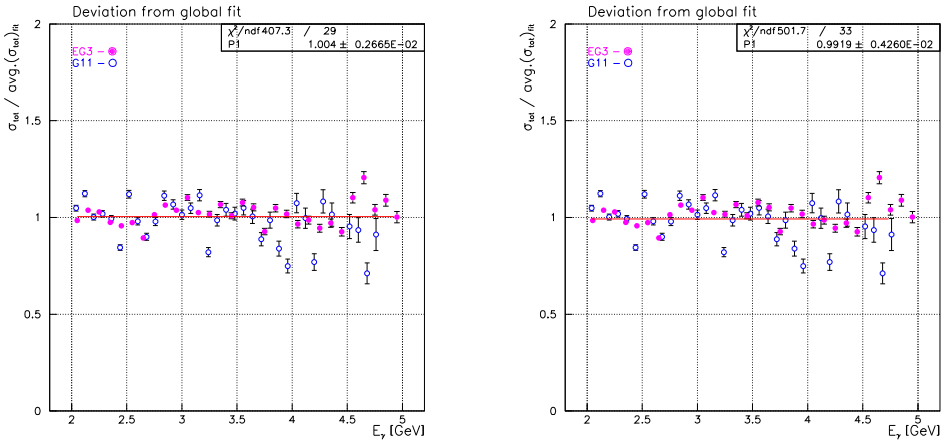

Figure 22: Ratio fits for 5.3 EG3 data (●) of 1.004, and G11 data (○) of 0.9919 between 2 GeV and 5 GeV .

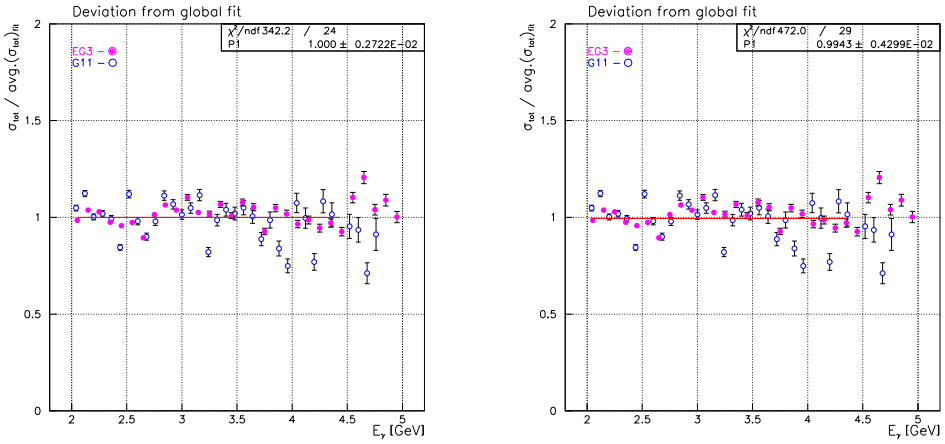

Figure 23: Ratio fits for 5.3 EG3 data (●) of 1.000, and G11 data (○) of 0.9943 below 4.5 GeV (untriggered region).

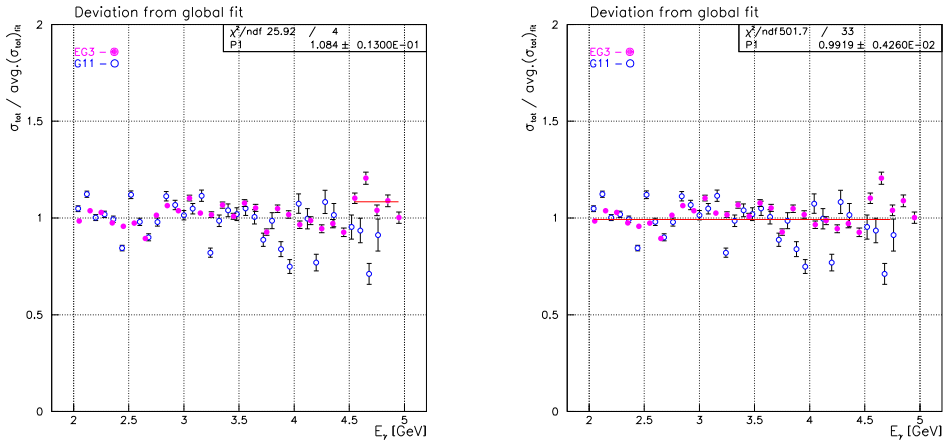

Figure 24: Ratio fits of EG3 (using 5.3 factor) and the G11 data. Above 4.5 GeV (left plot of EG3) and between 2 and 5 GeV (right plot for G11). The ratio between EG3 and the average fit is 1.084. The ratio between G11 and the average fit is 0.9919. The ratios are compared to the fit of the combined EG3/G11 data fits.

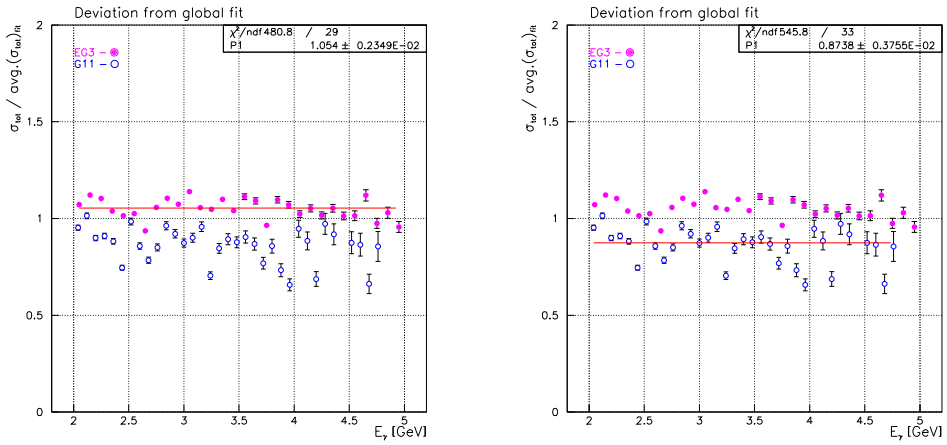

Figure 25: Ratio fits for 6.4 EG3 data (●) of 1.054, and G11 data (○) of 0.8738 between 2 GeV and 5 GeV .

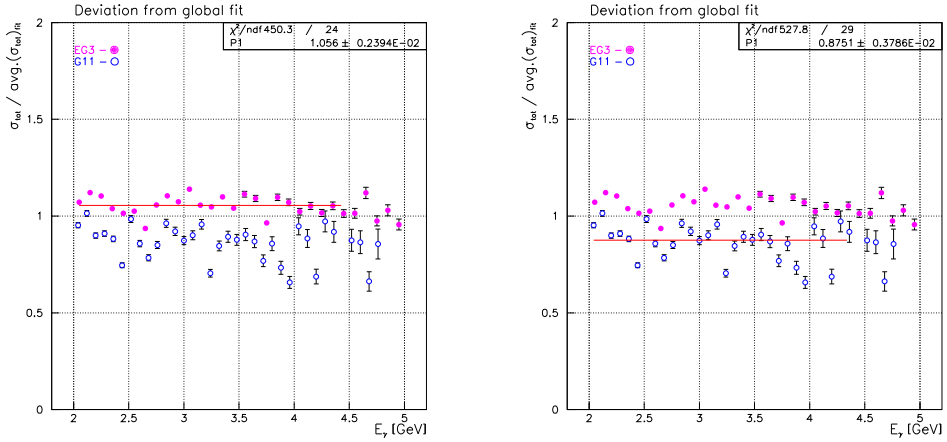

Figure 26: Ratio fits for 6.4 EG3 data (●) of 1.056, and G11 data (○) of 0.8751 below 4.5 GeV (untriggered region).

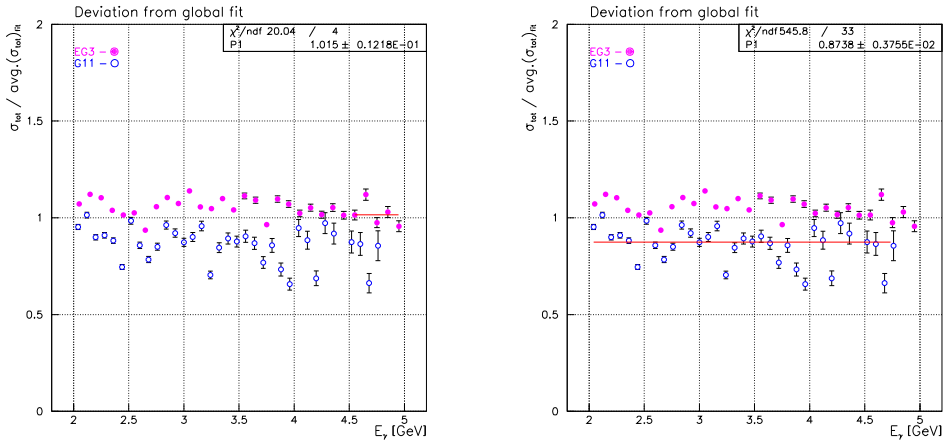

Figure 27: Ratio fits of EG3 (using 6.4 factor) and the G11 data. Above 4.5 GeV (left plot of EG3) and between 2 and 5 GeV (right plot for G11). The ratio between EG3 and the average fit is 1.015. The ratio between G11 and the average fit is 0.8738. The ratios are compared to the fit of the combined EG3/G11 data fits.

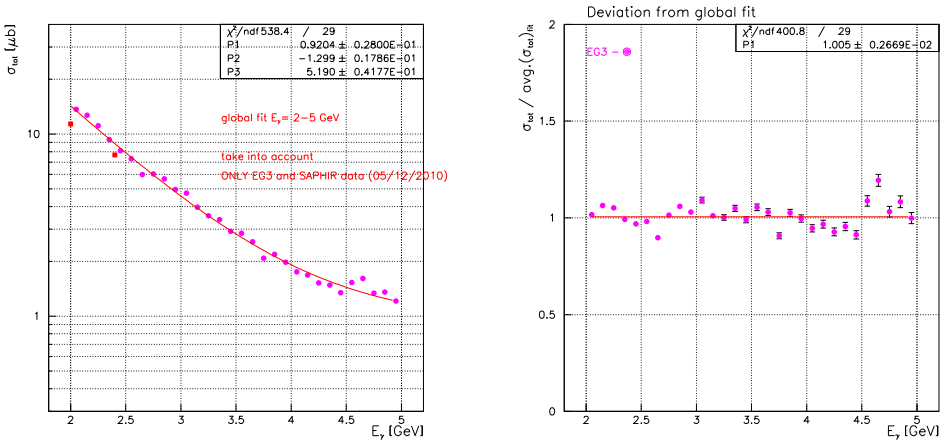

Figure 28: Comparison of EG3 (●) , and SAPHIR (■) data fit and ratio.

Table 3: Overall uncertainties for the cross section data with an average fit for comparison of EG3 to G11 overall, from 2 - 4.5 GeV, and from 4.5 - 5 GeV, and also for EG3 to SAPHIR over the limited range that SAPHIR covers. Uncertianties were calculated from Figure 22 - 27 and agreements are given for applying the 5.3 and the 6.4 untriggered tagged region correction value.

Data Sets (fit range)	Δ^{++} Channel (untagged factor = 5.3)	Δ^{++} Channel (untagged factor = 6.4)
EG3/G11(2-5 GeV)	$1\% \pm 1\%$	$18\% \pm 0.4\%$
EG3/G11(2-4.5 GeV)	$1\% \pm 1\%$	$18\% \pm 0.4\%$
EG3(4.5-5 GeV)/G11(2-5 GeV)	$9\% \pm 2\%$	$14\% \pm 1\%$
EG3/SAPHIR	$< 10\%$	$< 5\%$

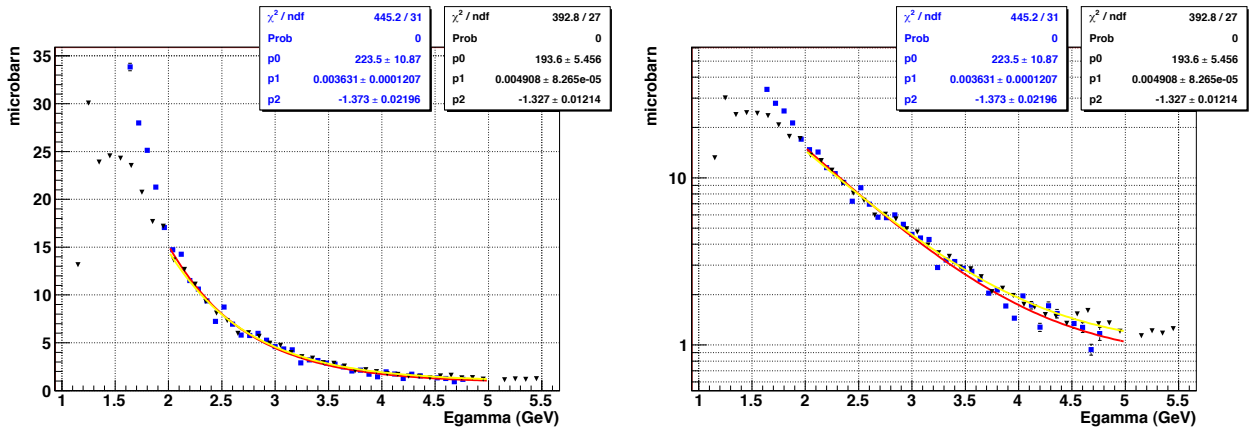

Figure 29: Comparison of EG3 (▼) , and G11 (■) data fit from 2 to 5 GeV. EG3 data set contains untagged triggered region correction factor of 5.3.

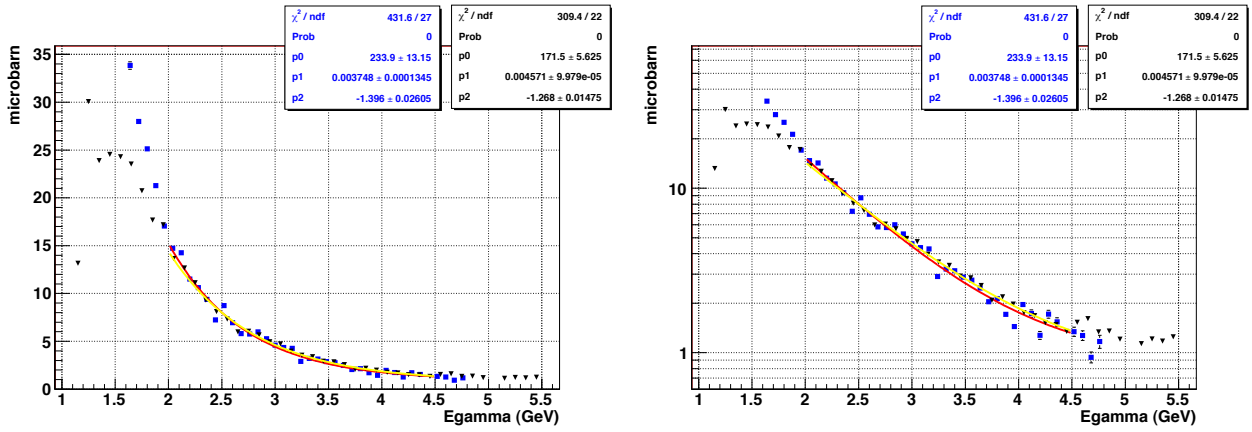

Figure 30: Comparison of EG3 (▼) , and G11 (■) data fit from 2 to 4.5 GeV. EG3 data set contains untagged triggered region correction factor of 5.3.

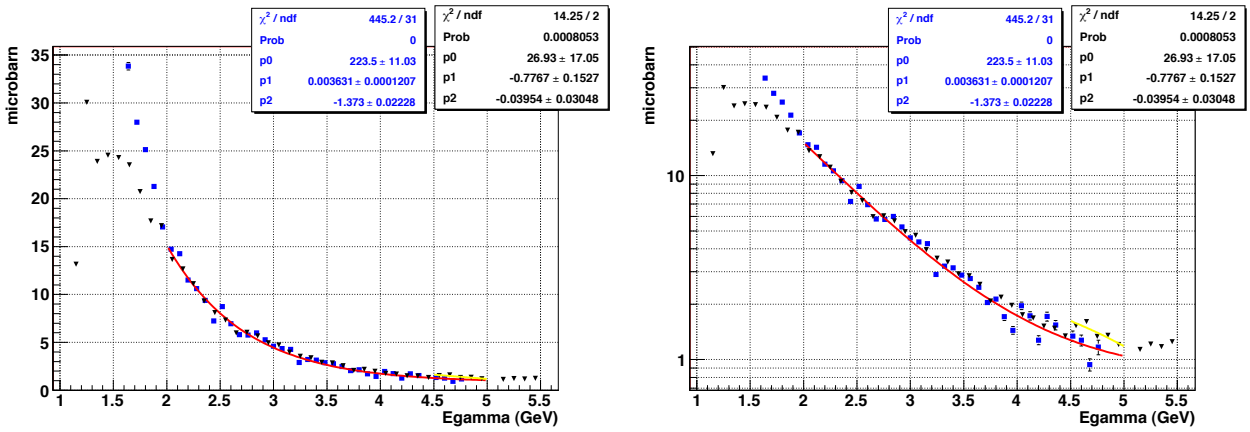

Figure 31: Comparison of EG3 (▼) , and G11 (■) data fit 4.5 to 5 GeV. EG3 data set contains untagged triggered region correction factor of 5.3. Here we compare the EG3 trigger region to the G11 full range, since the full range of the G11 data set is also the trigger region.

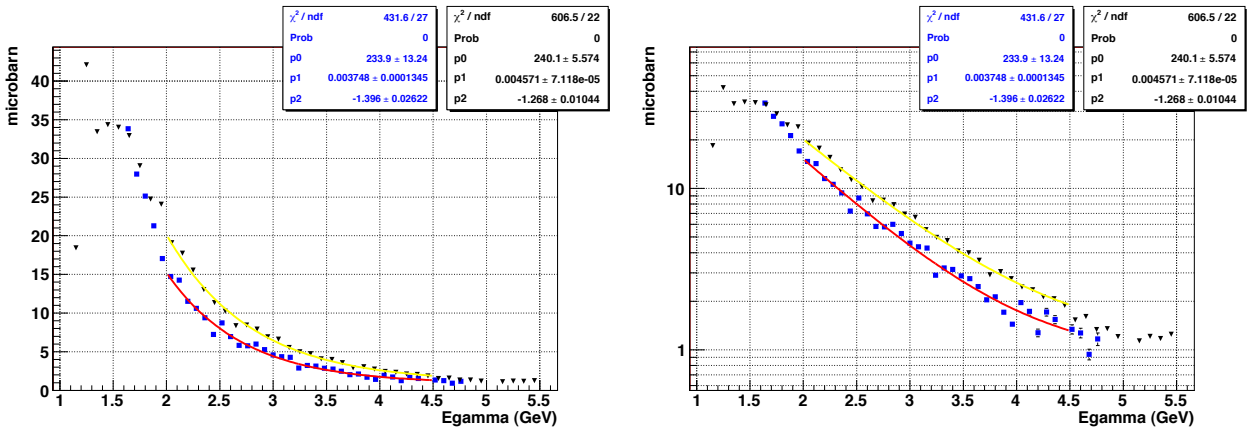

Figure 32: Comparison of EG3 (▼) , and G11 (■) data fit 2 to 5 GeV. EG3 data set contains untagged triggered region correction factor of 6.4.

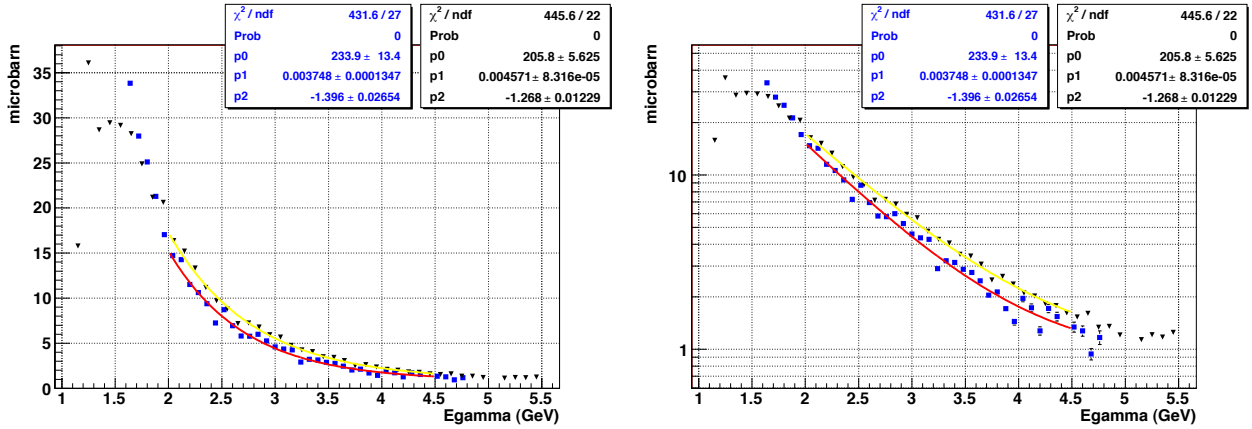

Figure 33: Comparison of EG3 (▼) , and G11 (■) data fit 2 to 4.5 GeV. EG3 data set contains untagged triggered region correction factor of 6.4.

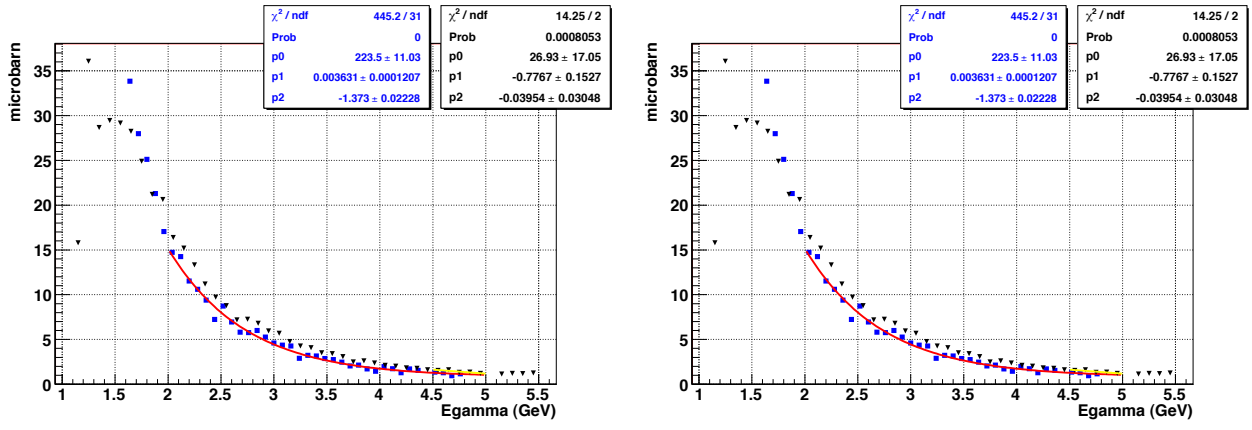

Figure 34: Comparison of EG3 (▼) , and G11 (■) data fit 4.5 to 5 GeV. EG3 data set contains untagged triggered region correction factor of 6.4. Here we compare the EG3 trigger region to the G11 full range, since the full range of the G11 data set is also the trigger region.

6 Summary

The reaction, $\gamma d \rightarrow p\pi^+\pi^- n$ was studied using tagged photons and the CLAS detector in Hall B at Jefferson Lab. The Δ^{++} was identified by observing its $p\pi^+$ decay products using skimmed data files from the EG3 data run. Preliminary cross sections have been extracted and are presented in this note. For the extraction, several methods were investigated and utilized to account for inefficiencies caused by the detector, event selection, and systematic uncertainties. The current analysis provides vital information into the trigger efficiency of the EG3 trigger and measure the same cross section as the G11 experimental group. The normalization of the data proved promising results and displayed consistency throughout all checks. We found that we could normalize the untriggered range of our data by using a single constant factor. We also discovered a vital piece to the data correction in that the trigger efficiency correction was lacking in the analysis. This factor is not only needed for the overall data correction, but it is also dependent on the final state particle selection under inverstigation.

The normalization and trigger efficiency study provided great insight and results in comparison to G11 CLAS data and also SAPHIR world data. From the final results we see that the systematic error of the cross section is dominated by the fit of the Δ^{++} yield, the untriggered tagged photon correction, and the trigger efficiency correction. In our Δ^{++} production comparison with other data, which is summarized in Table 3, we see an overall agreement with world data (SAPHIR) and G11 results for the $p\pi^+\pi^-$ skimmed correction within 18% agreement. Though we are confident in our findings thus far, we are still performing studies to test the consistencies of unexpected corrections we made to the data such as the untagged trigger region correction and the trigger efficiency.

References

[1] E. Pasyuk. Energy loss corrections for charged particles in clas. CLAS-NOTE 2007-016, (2007).

[2] H. Egiyan, M. Holtrop, and E. Smith. "Upper Limits for the Photoproduction Cross Section for the $\Phi^{--}(1862)$ Pentaquark State in $\Xi^-\pi^-$ Decay Channel Using EG3 Data. CLAS-ANALYSIS-2009-104, (2009).

[3] R. Gothe, H. Holtrop, E.S. Smith, and S. Stepanyan. Spokespersons for Search for "Exotic Cascades with CLAS Using an Untagged Virtual Photon Beam". JLab Experiment E-04-010, (2004).

[4] J. Barth, W. Braun, C. Wu. Photoproduction of ρ^0-mesons and Δ-baryons in the reactions $\gamma p \rightarrow p\pi^+\pi^-$ at energies up to $\sqrt{s} = 2.6$ GeV. Euro. Phys. J. A **23**, 317-344 (2005).

[5] P. Mattione. Kinematic fitting of detached vertices. JLAB-PHY-07-643, May (2007).

[6] J. Ball and E. Pasyuk. Photon Flux Determination Through Sampling of "out-of-time" Hits with the Hall B Photon Tagger. CLAS-NOTE 2005-002, (2005).

[7] M. Battaglieri and R. De Vita, G11 hardware trigger and software reconstruction efficiency.

[8] M. Holtop. CLAS GEANT Simulation. $www.physics.unh.edu/maurik/gsim_info.shtml$.